

# Random Fields and the Partially-Paramagnetic State of $\text{CsCo}_{0.83}\text{Mg}_{0.17}\text{Br}_3$ : A Critical Scattering Study

J. van Duyn<sup>1</sup>, B.D. Gaulin<sup>1,3</sup>, M.A. Lumssen<sup>1</sup>, and W.J.L. Buyers<sup>2,3</sup>

<sup>1</sup>Department of Physics and Astronomy, McMaster University, Hamilton, Ontario, L8S 4M1, Canada

<sup>2</sup>Neutron Program for Materials Research, National Research Council,  
Chalk River Laboratories, Chalk River, K0J 1J0, Canada and

<sup>3</sup>Canadian Institute for Advanced Research, 180 Dundas Street W, Toronto, ON, M5G 1Z8, Canada  
(Dated: April 14, 2024)

Critical neutron scattering measurements have been performed on  $\text{CsCo}_{0.83}\text{Mg}_{0.17}\text{Br}_3$ , a dilute stacked triangular lattice (STL) Ising antiferromagnet (AF). A two component lineshape associated with the critical fluctuations appears at a temperature coincident with  $T_{N1}$  observed in pure  $\text{CsCoBr}_3$ . Such scattering is indicative of fluctuations in prototypical random field Ising model (RFIM) systems. The random field domain state arises in this case due to geometrical frustration within the STL Ising AF, which gives rise to a 3 sublattice Neel state, in which one sublattice is disordered. Magnetic vacancies nucleate AF domains in which the vacancies reside on the disordered sublattice thereby generating a RFIM state in the absence of an applied magnetic field.

Geometrically frustrated magnetic materials have been of intense recent interest, in part due to the diversity in the exotic ground states that they display [1]. These span the range from complex non-collinear Neel states, to disordered co-operative paramagnetic and spin liquid states, to spin glass-like states in the presence of little or no chemical disorder. Among the exotic magnetic states known to exist are partially-paramagnetic Neel states, characterized as multi-sublattice antiferromagnets, in which one of the sublattices in this long range ordered structure remains paramagnetic. This unusual structure occurs in several magnetic materials made up of triangular planes, including the stacked triangular lattice Ising antiferromagnetic insulators  $\text{CsCoBr}_3$  [2] and  $\text{CsCoCl}_3$  [3], as well as the hexagonal intermetallic compound  $\text{UNi}_4\text{B}$  [4].

A striking feature of the phase behavior of  $\text{CsCoBr}_3$  and  $\text{CsCoCl}_3$  is their extreme sensitivity to the presence of non-magnetic impurities on the magnetic Co site. Neutron scattering work on  $\text{CsCo}_{1-x}\text{Mg}_x\text{Cl}_3$  by Nagler et al. [5] and on  $\text{CsCo}_{1-x}\text{Mg}_x\text{Br}_3$  by Rogge et al. [6] show that 17% dilution of the cobalt sites with non-magnetic magnesium appears to wipe out at least two (and possibly three) long range ordered states which pure  $\text{CsCoCl}_3$  displays below  $T_{N1} = 21\text{ K}$  [3], and which pure  $\text{CsCoBr}_3$  displays below  $28\text{ K}$  [2]. This is surprising as 3 dimensional lattices support percolating long range order to 75% dilution. [7].

In this letter, we report on a critical neutron scattering study of single crystal  $\text{CsCo}_{0.83}\text{Mg}_{0.17}\text{Br}_3$ . We show that the critical fluctuations contain two components, the narrower of which (in  $Q$ -space) displays an onset at a temperature co-incident with  $T_{N1}$  of pure  $\text{CsCoBr}_3$ ,  $28\text{ K}$ . Two distinct components to the fluctuations are easily observed over the approximate temperature interval for which pure  $\text{CsCoBr}_3$  exhibits the exotic partially-paramagnetic, 3-sublattice Neel state. We argue that this two component lineshape is characteristic of a domain state typical of the Random Field Ising Model (RFIM),

and which is generated by the presence of quenched magnetic vacancies and the paramagnetic sublattice.

RFIMs occupy interesting and important territory within the physics of disordered media [8]. Within this model the disorder arises due to random local symmetry breaking, as opposed to random interactions and frustration, which drives the physics of conventional spin glasses [9]. The RFIM is known to describe well the properties of magnetically-dilute Ising antiferromagnets in the presence of magnetic fields [10, 11, 12, 13], as well as a wide class of other disordered materials, such as, for example, phase separating fluids in the presence of gels [14].

Imry and Ma first considered the effects of a ferromagnetic Ising system in the presence of a site-random magnetic field, and argued that the random fields would destroy the long range order of such a classical system for dimensions less than 4 [15]. Fishman and Aharony later argued that magnetically dilute Ising antiferromagnets in the presence of a uniform magnetic field were isomorphous to the Imry-Ma scenario [16]. This was important as not only do site-random antiferromagnets occur in nature, but it is easy to apply an external magnetic field and thereby tune the amplitude of the random field.

Systematic studies of such site-random Ising antiferromagnets have been carried out for both three dimensional materials (such as  $\text{CoZn}_{1-x}\text{F}_2$  [10],  $\text{MnZn}_{1-x}\text{F}_2$  [11], and  $\text{FeZn}_{1-x}\text{F}_2$  [12]) as well as quasi-two dimensional systems (such as  $\text{Rb}_2\text{Co}_{0.7}\text{Mg}_{0.3}\text{F}_4$  [13]). While some open questions remain, it is clear that the field-cooled state at low temperatures corresponds to a system broken up into many relatively small domains. A characteristic signature of such a state in neutron scattering experiments is a two-component lineshape in wave vector, with a sharp and a broad component, as opposed to the single-component lineshape corresponding to, say, Omslein-Zemike fluctuations [17]. Such a two-component lineshape, however, was inferred from the results of fitting the neutron lineshapes to an appropriate addition of two

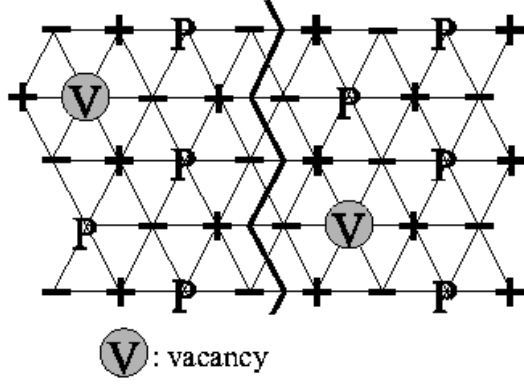


FIG. 1: Role of non-magnetic atoms in generating a random field domain state in  $\text{CsCo}_{0.83}\text{Mg}_{0.17}\text{Br}_3$

terms.

$\text{CsCo}_{0.83}\text{Mg}_{0.17}\text{Br}_3$  belongs to the  $\text{ABX}_3$  family of antiferromagnetic (AF) insulators [18]. The interest in these materials stems from the quasi-one-dimensional nature of their magnetic interactions, as well as their geometrically frustrated cooperative behaviour. Pure  $\text{CsCoBr}_3$  is an example of an Ising-like antiferromagnet on a stacked triangular lattice [2]. It crystallizes in the hexagonal space group  $P6_3/mmc$ , with low temperature lattice parameters  $a = 7.45$  and  $c = 6.30$  Å. The  $\text{Co}^{2+}$  ions possess spin- $\frac{1}{2}$  magnetic moments, which are aligned along the hexagonal  $c$  direction, and lie on a simple hexagonal lattice. Inelastic neutron scattering studies have shown that this material is described by the following spin Hamiltonian [19]:

$$H = \sum_{i(e)}^X (2JfS_i^z S_{i+1}^z + (S_i^x S_{i+1}^x + S_i^y S_{i+1}^y)g) + h_0 S_i^z (-1)^i + 2J^0 \sum_{j(ab)}^X S_i^z S_j^z \quad (1)$$

where  $J = 1.62$  THz,  $J' = 0.0096$  THz and  $g = 0.137$ . The dominant AF interactions along the  $c$ -axis result in quasi-one dimensional behaviour over an extended temperature regime. At sufficiently low temperatures, however, the weaker  $ab$ -plane interactions cause two or possibly three, magnetic phase transitions to three dimensional long range ordered Neel states [2, 20]. The first phase transition, from the paramagnetic state to a long range ordered, but partially-paramagnetic state, occurs at  $T_{N1} = 28.3$  K. This state is characterized by three sublattices, in which two out of every three spins on triangular plaquettes are ordered antiferromagnetically, while the third remains disordered. This is shown as +, - and P in Fig 1. The ordering triples the periodicity within the  $ab$ -plane, giving rise to magnetic Bragg reflections of the form  $(\frac{1}{3}, \frac{1}{3}, l)$  with  $l$  odd. Below 13 K the paramagnetic sublattice orders fully, either (+) up or down (-), to form a ferrimagnetic sheet within the  $ab$ -plane. The net moment within this ferrimagnetic sheet orders alter-

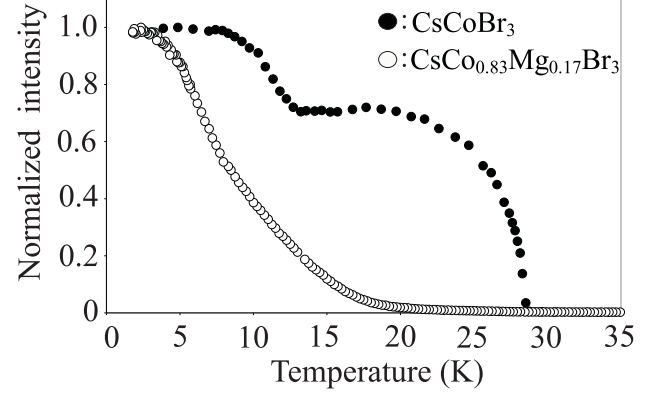


FIG. 2: Peak intensity of the magnetic  $(\frac{2}{3}, \frac{2}{3}, l)$  and  $(\frac{4}{3}, \frac{4}{3}, l)$  Bragg reflection of  $\text{CsCoBr}_3$  and  $\text{CsCo}_{0.83}\text{Mg}_{0.17}\text{Br}_3$  respectively as a function of temperature.

nately from  $ab$ -plane to  $ab$ -plane, so as to produce an antiferromagnetic structure, with no net magnetic moment. An intermediate magnetically-ordered structure may exist between 18 K and 13 K, in which the paramagnetic sublattice gradually orders.

Classical Ising antiferromagnets on stacked triangular lattices have been studied extensively by Landau-Ginsburg-Wilson [21] and Monte Carlo techniques [22]. The high and low temperature long range ordered states are accounted for by all theoretical models.

The argument by which the combination of a partially-paramagnetic Neel state and magnetic vacancies generate a random field domain state is illustrated in Fig. 1. These quenched vacancies will preferentially nucleate domains in which the vacancies are coincident with the paramagnetic sublattice so as to minimize the loss of exchange energy. Two such domains are depicted in Fig. 1, with a domain wall running between them. In the absence of the paramagnetic sublattice, the vacancies are co-incident with either up or down sublattices, and only break symmetry between the two in the presence of an externally applied longitudinal magnetic field; the Fisher-Aharony scenario [16].

The critical neutron scattering study was carried out on the N5 triple axis spectrometer, operated in two axis mode, at the NRU reactor of Chalk River Laboratories. The high quality single crystal was the one studied by Rogge et al. [6]. Neutrons of wavelength 2.37 Å were reflected from the (0;0;2) planes of a pyrolytic graphite (PG) monochromator. A PG filter was placed between the monochromator and sample to remove higher order contamination. The sample, mounted in a  $\text{He}^4$  cryostat, was oriented with its  $(h;h;l)$  plane in the horizontal scattering plane. Collimation of 0.19° in the incident beam and 0.25° in the diffracted beam was used to achieve relatively high  $Q$  resolution.

The temperature dependence of the Bragg peak intensities in both pure  $\text{CsCoBr}_3$  and dilute  $\text{CsCo}_{0.83}\text{Mg}_{0.17}\text{Br}_3$  is shown in Fig. 2. The square of the

order parameters were taken to be proportional to the peak intensities at the magnetic Bragg reflection,  $(\frac{2}{3}; \frac{2}{3}; 1)$  for  $\text{CsCoBr}_3$  and  $(\frac{4}{3}; \frac{4}{3}; 1)$  for  $\text{CsCo}_{0.83}\text{Mg}_{0.17}\text{Br}_3$ .

While more complete than that reported by Rogge et al. [6], the  $\text{CsCo}_{0.83}\text{Mg}_{0.17}\text{Br}_3$  order parameter squared presented in Fig. 2 reproduces the key characteristics of the earlier measurements. The Bragg intensity displays upwards curvature down to at least 5 K, and the clear phase transitions in pure  $\text{CsCoBr}_3$  at 28.3 K and 13 K are not evident. Mean field behavior would predict this intensity to grow linearly with decreasing temperature as  $(T_c - T)^2$  with  $\beta = 0.5$ . Typical three dimensional critical behavior would give  $\frac{1}{3}$ . Pronounced downwards curvature in the Bragg intensity as a function of temperature would be expected, and indeed is observed in pure  $\text{CsCoBr}_3$  as shown in Fig. 2.

Similar order parameter measurements on  $\text{CsCo}_{0.83}\text{Mg}_{0.17}\text{Cl}_3$  by Nagler et al. [5] also show upwards curvature to the Bragg intensity as a function of temperature to temperatures below 5 K, and again no evidence of the  $T_{N1} = 21$  K observed in pure  $\text{CsCoCl}_3$ . While these earlier studies concluded phase transitions occur near 9 K and 6 K, for  $\text{CsCo}_{0.83}\text{Mg}_{0.17}\text{Br}_3$  and  $\text{CsCo}_{0.83}\text{Mg}_{0.17}\text{Cl}_3$  respectively, neither study showed compelling evidence for any phase transition above 5 K.

As a function of temperature, scans in  $h$  and  $l$  were performed through three ordering wavevectors:  $\mathbf{Q}_{\text{ord}} = (\frac{1}{3}; \frac{1}{3}; 1), (\frac{2}{3}; \frac{2}{3}; 1)$  and  $(\frac{4}{3}; \frac{4}{3}; 1)$ . As shown by the  $h$ -scans in Fig. 3 a sharp, albeit relatively weak component, additional to the broad critical fluctuations, appears below 28 K. This indicates that a broken symmetry has occurred very close to pure  $\text{CsCoBr}_3$ 's  $T_{N1}$ . Over the temperature range 28 K to 20 K, the scattering clearly displays a two component line shape.

The data were analysed by convoluting the scattering cross section with the measured 3-dimensional resolution function. The cross section, centered at each ordering wavevector, is described by the sum of a broad and a narrow Lorentzian, both having anisotropic widths. The calculated intensities included both the  $\text{Co}^{2+}$  magnetic form factor, and the neutron polarization factor, by which only components of momentum perpendicular to  $\mathbf{Q}$  contribute to the scattering.

The inverse correlation lengths within the  $ab$ -plane and along the  $c$ -axis were allowed to differ, accounting for the strong anisotropic nature of the AF interactions within this material; hence:

$$S(\mathbf{Q}) = \frac{A}{1 + \frac{q_a^2 + q_b^2}{2} + \frac{q_c^2}{c}} + \frac{B}{1 + \frac{q_a^2 + q_b^2}{2} + \frac{q_c^2}{c}} \quad (2)$$

where  $\frac{1}{\xi_{ab}} < \frac{1}{\xi_{ab}^0}$ ,  $\frac{1}{\xi_c} < \frac{1}{\xi_c^0}$ , and  $\mathbf{q} = \mathbf{Q} - \mathbf{Q}_{\text{ord}}$ . The inverse correlation lengths of the broad Lorentzian were allowed to refine, while those of the narrow one were held fixed (at  $\frac{1}{\xi_{ab}} = 0.00546$  and  $\frac{1}{\xi_c} = 0.00624 \text{ \AA}^{-1}$ , approximating their resolution limit). A complete fit to the data required

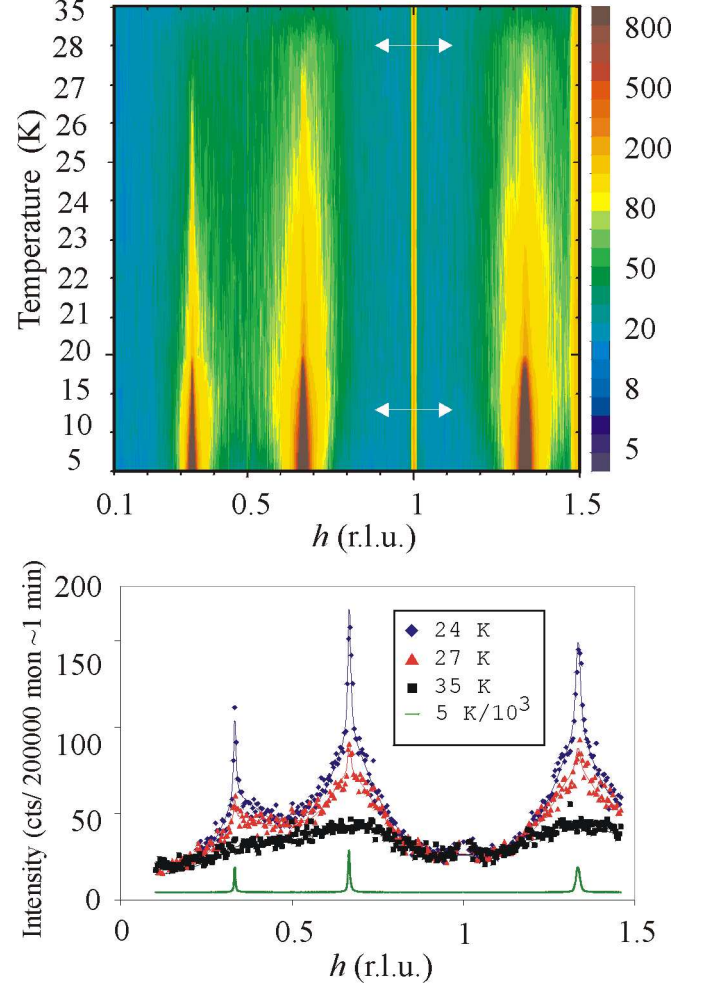


FIG. 3: (top) Scattering data along the  $(h; h; 1)$  direction at the 13 measured temperatures. The white arrows indicate the temperatures at which clear phase transitions are observed in pure  $\text{CsCoBr}_3$  (see Fig. 2). (bottom) Representative  $(h; h; 1)$  scans clearly showing the onset of a two-component line shape below  $T_{N1}$ . The solid lines are fits of the data to Eq. 2, convoluted with the experimental resolution. The bottom data set, scaled in intensity by a factor of  $10^3$ , shows that only the sharp component remains at 5 K.

adding two broad and relatively weak Lorentzians centered at wavevectors  $(\frac{1}{2}; \frac{1}{2}; 1)$  and  $(\frac{3}{2}; \frac{3}{2}; 1)$ , in addition to a constant background. This extra scattering originates from the domain walls within the  $ab$ -plane. A stable paramagnetic sublattice requires a net zero exchange field from its near neighbours (3 up (+) and 3 down (-) near neighbours). The domain wall regions therefore exclude the paramagnetic sublattice and reflect a local two sublattice structure (Fig. 1), giving rise to scattering at  $(\frac{h}{2}; \frac{h}{2}; 1)$  with  $h$  odd.

Figure 4 shows the temperature dependence of the refined parameters. The narrow component to the line shape turns on below 28 K, while the broad component extends above  $T_{N1}$ . Below 20 K the intensity of the narrow component rapidly increases, and the data can be

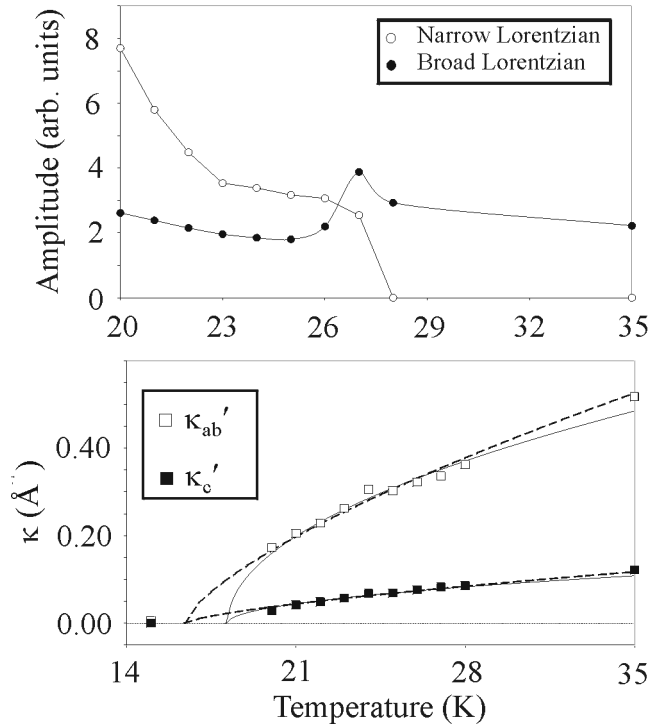


FIG. 4: (top) Temperature dependence of the amplitude of both the narrow and broad Lorentzians, resulting from fits shown in the bottom panel of Fig. 3. (Bottom), The temperature dependence of the inverse correlation lengths of the broad Lorentzian are shown along with fits to divergences in the correlation lengths, appropriate to both mean field theory ( $\nu = \frac{1}{2}$ ) and the 3D Heisenberg model ( $\nu = 0.707$ ), as described by Eq. 3

equally well described by a single component Lorentzian with anisotropic line widths.

To seek out a second, lower phase transition, we have fit the temperature dependence of the inverse correlation lengths of the broad component between 20 K and 28 K. This was fit to a standard critical divergence of the correlation lengths as:

$$\kappa_{ab;c}^{-1} = \frac{1}{\kappa_{ab;c}^0} (T - T_{N2})^{-\nu} \quad (3)$$

We fit with critical exponents ranging from a low of  $\frac{1}{2}$ , appropriate to mean field theory, to a high of 0.707 appropriate to the 3D Heisenberg model. These fits, shown in the bottom panel of Fig. 4, are consistent with a second phase transition occurring between 16 K and 18 K.

While a unique, quantitative analysis of the scattering below 20 K is difficult, examination of the qualitative features of the scattering in Fig. 3 is useful. The order parameter for  $\text{CsCo}_{0.83}\text{Mg}_{0.17}\text{Br}_3$  in Fig. 2 shows little or no indication of the 13 K transition in  $\text{CsCoBr}_3$ . However the  $(h, h, 1)$  scans in the top panel of Fig. 3 clearly show a narrowing in the diffuse scattering below 13 K,

indicating the onset of a true long range ordered state. We interpret this as a tendency towards full ordering of the paramagnetic sublattice below  $T_{N3} = 13$  K, thereby removing the driving force for the RFI M behavior in the absence of an applied magnetic field, that is the paramagnetic sublattice.

Our critical scattering study of  $\text{CsCo}_{0.83}\text{Mg}_{0.17}\text{Br}_3$  has resolved a longstanding mystery [5, 6] as to the extreme sensitivity of the long range ordered partially-paramagnetic Néel state to quenched magnetic vacancies. It also contrasts with very recent theoretical work on doped quasi-1D Heisenberg antiferromagnets [23]. Our results show that  $\text{CsCo}_{0.83}\text{Mg}_{0.17}\text{Br}_3$  still displays a symmetry breaking near pure  $\text{CsCoBr}_3$ 's  $T_{N1} = 28$  K, but that the system enters a RFI M domain state, and remains in such a state until sufficiently low temperatures that the paramagnetic sublattice orders, at approximately 13 K.

This work was supported by NSERC of Canada.

- 
- [1] for recent reviews see Magnetic Systems with Competing Interactions, edited by H.T. Diep (World Scientific, Singapore, 1994); P. Schier and A.P. Ramirez, Comments Condens. Matter Phys., 18, 21 (1996).
  - [2] W.B. Yelon, D.E. Cox and M. Eibschutz, Phys. Rev. B, 12, 5007 (1975).
  - [3] M. Mekata and K. Adachi, J. Phys. Soc. Japan, 44, 806 (1978).
  - [4] S.A.M. Mentink et al, Phys. Rev. Lett., 73, 1031 (1994).
  - [5] S.E. Nagler et al., J. Phys. C, 17, 4819 (1984).
  - [6] R.B. Rogge et al., J. Appl. Phys., 73, 6451 (1993).
  - [7] P.M. Chaikin and T.C. Lubensky, Principles of Condensed Matter Physics, (Cambridge, 1995.)
  - [8] D.P. Belanger, in Spin Glasses and Random Fields, edited by A.P. Young (World Scientific, Singapore, 1998); R.J. Birgeneau, J. Magn. Magn. Mater., 177, 1 (1998).
  - [9] J.A. Mydosh, Spin Glasses (Taylor and Francis, 1993)
  - [10] M. Hagen et al., Phys. Rev. B, 28, 2602 (1983).
  - [11] R.A. Cowley et al., Phys. Rev. B, 30, 6650 (1984).
  - [12] R.A. Cowley et al. Z. Phys B, 58, 15 (1985).
  - [13] R.J. Birgeneau et al., Phys. Rev. B, 28, 1438 (1983).
  - [14] B.J. Frisken, D.S. Cannell, M.Y. Lin and S.K. Sinha, Phys. Rev. E, 51, 5866 (1995); B.J. Frisken, F. Ferri and D.S. Cannell, Phys. Rev. E, 51, 5922 (1995).
  - [15] Y. Imry and S.K. Ma, Phys. Rev. Lett., 35, 1399 (1975).
  - [16] S.F. Ishman and A. Aharony, J. Phys. C, 12, L729 (1979).
  - [17] R.A. Cowley, in Methods of Experimental Physics, 23C, Neutron Scattering, 1, Academic Press (1987).
  - [18] M.F. Collins and O.A. Petrenko, Can. J. Phys., 75, 605 (1997).
  - [19] S.E. Nagler, et al., Phys. Rev. B, 27, 1784 (1983); *ibid.*, 28, 3873 (1983).
  - [20] A. Farkas, B.D. Gaulin, Z. Tun and B. Briat, J. Appl. Phys., 69, 6167 (1991).
  - [21] D. Blankstein et al., Phys. Rev., 29, 5250 (1984); M.L. Plumer and A. Caille, J. Appl. Phys., 70, 5961 (1991).
  - [22] M.L. Plumer et al., Phys. Rev. B, 47, 14312 (1993); A. Bunker, B.D. Gaulin, and C. Kallin, Phys. Rev. B, 48, 15861 (1993).

[23] S. Eggert et al., Phys. Rev. Lett., 89, 047202, 2002.